

Search for Ξ^{*-} , Σ^{*-} , and Ω^- production by negative hyperons on nuclei

V. Hungerbühler,* R. Majka, J. N. Marx, P. Némethy, J. Sandweiss, W. Tanenbaum, and W. J. Willis[†]
Yale University, New Haven, Connecticut 06520[‡]

M. Atac, S. Ecklund, P. J. Gollon, J. Lach, J. MacLachlan, A. Roberts, R. Stefanski, and D. Theriot
Fermi National Accelerator Laboratory, Batavia, Illinois 60510[§]

C. L. Wang
Brookhaven National Laboratory, Upton, New York 11973

W. Cleland, E. Engels, Jr., D. I. Lowenstein,[¶] N. Scribner,** and J. Thompson
University of Pittsburgh, Pittsburgh, Pennsylvania 15260^{††}

(Received 6 May 1974)

The reactions of 24.6-GeV/c Σ^- and Ξ^- incident on a scintillator target were studied in a counter-spark chamber experiment. Upper limits on the production cross sections of Σ^{*-} resonances which decay into $\Lambda^0\pi^-$ and Ξ^{*-} resonances which decay into Λ^0K^- were obtained. A single Ω^- that was produced in the scintillator target has been observed, corresponding to a 115- $\mu\text{b/nucleon}$ production cross section if produced by a Ξ^- . The $\Lambda^0\pi^-$ mass spectrum was found to be consistent with a Deck-type threshold enhancement.

We report the results of a search for hyperon resonance and Ω^- production by negative hyperons incident on a plastic scintillator target:

$$\left\{ \begin{matrix} \Sigma^- \\ \Xi^- \end{matrix} \right\} + \text{nucleus} \rightarrow \left\{ \begin{matrix} \Sigma^{*-} \\ \Xi^{*-} \\ \Omega^- \end{matrix} \right\} + \text{anything.}$$

The experiment was performed in the high-energy negative hyperon beam at the Alternating Gradient Synchrotron (AGS) of the Brookhaven National Laboratory. Scintillator and spark-chamber arrays were used to identify the final states

$$\begin{matrix} \Lambda^0\pi^- \\ \searrow \\ p\pi^- \end{matrix} \quad \text{and} \quad \begin{matrix} \Lambda^0K^- \\ \searrow \\ p\pi^- \end{matrix}$$

from resonance or Ω^- decay, and to measure their effective mass.

The hyperon beam is a short, curved magnetic channel that delivers fluxes of approximately 200 Σ^- and 2 Ξ^- per 1.5×10^{11} interacting protons, at a momentum of 24.6 GeV/c. Figure 1 is a plan view of the hyperon beam and detection apparatus, which is described in detail elsewhere.¹ Beam particles of mass less than 1 GeV/c² are tagged and vetoed by a threshold Čerenkov counter (C_B) which forms part of the magnetic channel. A high-pressure, high-resolution ($\sigma < 100 \mu\text{m}$) magnetostrictive spark chamber² measures the momentum (to $\pm 1\%$) and direction (to $\pm 0.5 \text{ mrad}$) of hyperons emerging from the channel. Small scintillation counters (B) define the beam. A hole veto counter (V_H) downstream of the high-resolution spark chambers discriminates against beam halo and upstream hyperon decays.

A $5 \times 5 \times 25$ -cm-long plastic scintillator production target follows the high-resolution spark chambers. The pulse height from this target is recorded for each event to help differentiate between diffractive and nondiffractive production processes.

Located downstream from the 1.5-m-long decay region is a double magnetic spectrometer with conventional magnetostrictive spark chambers. The first spectrometer analyzes the relatively low-momentum ($< 10 \text{ GeV}/c$) π^- and K^- mesons from the target or from hyperon decays. The second spectrometer measures the momentum of the high-energy protons from $\Lambda^0 \rightarrow p\pi^-$ decays. The field integrals of the two magnets are 13 kG m and 26 kG m, respectively, so that particle momenta are typically determined to between 2% and 5%. A counter hodoscope (S) between the spectrometer magnets serves to trigger on one or more slow negative particles. Two proton counters (P) and an iron-scintillator calorimeter (PC) define a proton trigger. The calorimeter rejects background muons, which can otherwise simulate good triggers. A large phase-space threshold Čerenkov counter between the two spectrometer magnets separates $\Lambda^0\pi^-$ from Λ^0K^- final states. This counter, which is filled with N_2O at atmospheric pressure,³ is sensitive to pions and kaons with momenta above 4.8 GeV/c and 16.8 GeV/c, respectively, and is therefore used to separate π^- from K^- in the momentum range of 5 to 12 GeV/c.

The trigger for either final state coming from the interaction of an incident hyperon is

$$\bar{C}_B \cdot B \cdot \bar{V}_H \cdot S \cdot P \cdot PC.$$

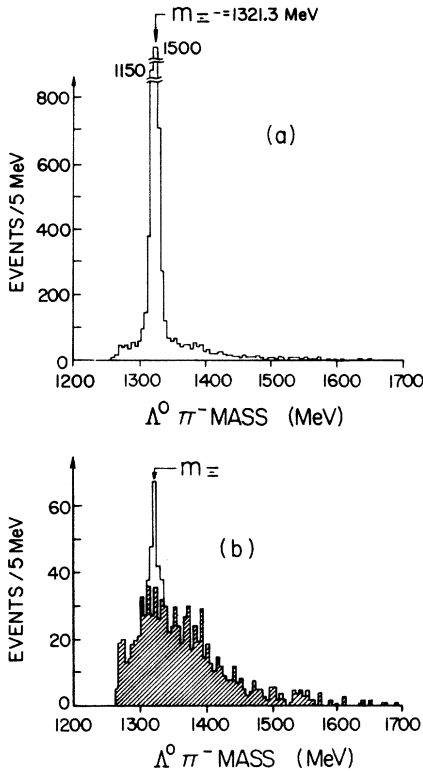


FIG. 3. (a) Mass distribution of $\Lambda^0\pi^-$ states with decay vertex in the scintillator target. (b) Unshaded histogram: mass distribution of the above events after requiring at least a 5-mrad angle between the incident hyperon momentum and the $\Lambda^0\pi^-$ momentum. Shaded histogram: the same distribution after the subtraction of background Ξ^- peak determined from decays *downstream* of the scintillator target.

is thus seen to be dominated by beam Ξ^- 's. In the analysis, a minimum angle requirement of 5 mrad between the momentum vector of the incident hyperon and that of the outgoing $\Lambda^0\pi^-$ system serves to discriminate against the beam Ξ^- . Figure 3(b) shows the resulting spectrum. We interpret the

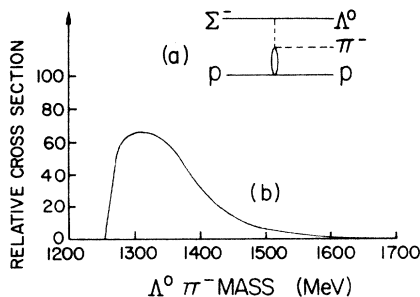


FIG. 4. (a) Deck-effect diagram for $\Sigma^-p \rightarrow \Lambda^0\pi^-p$. (b) Monte Carlo prediction of $\Lambda^0\pi^-$ invariant mass distribution due to Deck effect. Note the similarity to the observed spectrum shown as the shaded histogram in Fig. 3(b).

remaining Ξ^- peak as those beam Ξ^- 's which scattered elastically in the scintillator target. Events with a vertex downstream of the target show the cascade peak only.

There is no evidence for the Σ^{*-} resonances in the spectrum from the target [Fig. 3(b)]. After we subtract the remnant beam cascades as determined from the number seen decaying in the decay region, a broad enhancement remains at the mass threshold [shaded region in Fig. 3(b)]. A Monte Carlo calculation, starting with the simplest Deck-effect¹ matrix element [Fig. 4(a)] and simulating the acceptance of our apparatus, gives the predicted invariant mass spectrum shown in Fig. 4(b). The Deck-effect prediction closely resembles the shape of our data [shaded portion of Fig. 3(b)]. The inclusion of other Deck diagrams would not change this result since the predicted shape of the mass distribution is strongly influenced by our de-

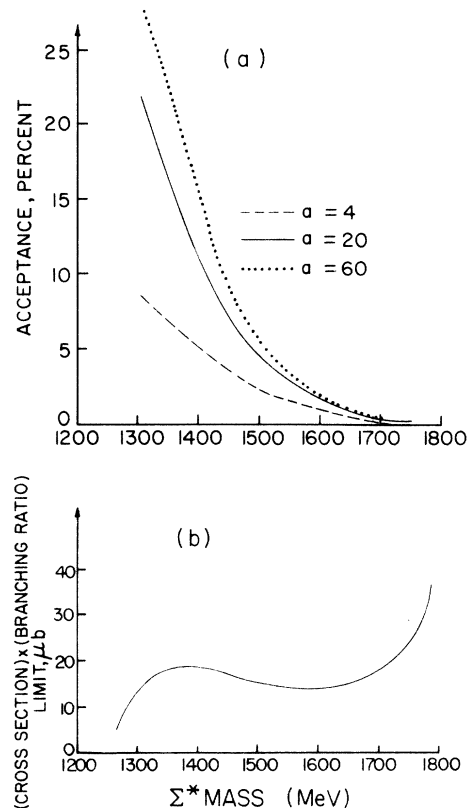


FIG. 5. (a) Acceptance of the apparatus as a function of resonance mass for $\Lambda^0\pi^-$ final states produced within the target. The three curves illustrate different assumed production cross sections, $d\sigma/dt \propto e^{at}$, where $a=4$ for nondiffractive Σ^{*-} production, $a=20$ for diffractive excitation on protons, and $a=60$ for diffractive excitation on ^{12}C . (b) Upper limit (90% confidence level) on the cross section for the production of Σ^{*-} which decay into $\Lambda^0\pi^-$, assuming $d\sigma/dt \propto e^{at}$ and a resonance width of 10 MeV.

tection efficiency, which is limited by the magnet apertures and decreases rapidly above 1400 MeV, as shown in Fig. 5(a). (The reason for this strong dependence of detection efficiency on resonance mass is that the spectrometers were designed for use in studies of hyperon production⁵ and leptonic decays.⁶) Figure 5(b) shows the upper limit on the cross section for resonance production of Σ^{*-} as a function of the Σ^{*-} mass.

The absence of a signal from the $\Sigma^{*}(1385)$ resonance is an interesting feature of the data. We put an upper limit (90% confidence level) of $80 \mu\text{b}$ on the production of this resonance, assuming a width of 40 MeV. Its absence may be due to the fact that the production of the $\Sigma^{*}(1385)$ from a Σ^{-} requires unnatural spin-parity exchange, as well as the exchange of SU_3 quantum numbers.⁷ Either of these factors can prevent $\Sigma^{*}(1385)$ production by Pomeron exchange. Production of $\Sigma^{*}(1385)$ by π exchange is possible, but the cross section for this process is small at the present energies.

One aim of this experiment was to detect the production of the strange SU_3 analogs of the $N^{*}(1470)$. The masses of such states, if they exist, may well be beyond the acceptance of this apparatus. If not, then either the production or the two-body decay of these states must be suppressed. The inhibition of such two-body decays is predicted by a quark model of Lipkin.⁸

Candidates for Ξ^{*-} resonances and Ω^{-} production $\Lambda^0 K^{-}$ final states were selected by requiring that the meson that is not from the Λ^0 decay be within the geometric acceptance and valid momentum range of the N_2O Čerenkov counter. This counter was then used as a pion veto. Figure 6(a) shows the apparatus acceptance as a function of Ξ^{*-} mass. Previous searches⁹ using K^{-} beams have not observed any states $\Xi^{*-} \rightarrow \Lambda^0 K^{-}$ with masses below 1820 MeV, which is above our sensitive mass region. However, it was felt that such lower mass states might be produced more readily by diffractive processes, just as πp and diffractive pp processes favor the production of different groups of N^{*} states.

No evidence was found for $\Lambda^0 K^{-}$ production in those events which had vertices in the scintillator target. Figure 6(b) shows the experimental upper limit on the cross section for the production of a single Ξ^{*-} in our mass region.

Events with a $\Lambda^0 K^{-}$ vertex in the decay region were analyzed for Ω^{-} decays since there was no background from target excitations in this region. One possible Ω^{-} event was found in this data sample. This event, which was produced in the scintillator target, has a reconstructed Λ^0 mass of $1118 \text{ MeV}/c^2$ and a reconstructed $p\pi^{-}K^{-}$ mass of $1676 \text{ MeV}/c^2$. A large pulse height was observed

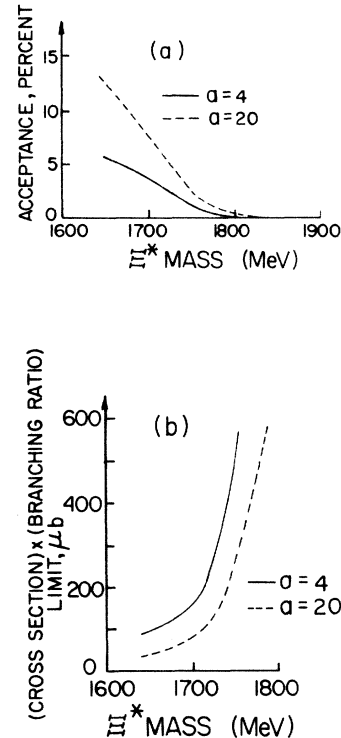


FIG. 6. (a) Acceptance of the apparatus as a function of Ξ^{*-} resonance mass for $\Lambda^0 K^{-}$ final states produced within the target. Two assumed production cross sections of the form $d\sigma/dt \propto e^{at}$ are shown. (b) Upper limits (90% confidence level) on the cross section for the production of Ξ^{*-} which decay into $\Lambda^0 K^{-}$. The same two production models are considered.

in the target scintillator with a large ($7.36 \text{ GeV}/c$) imbalance in longitudinal momentum. These signals are characteristic of a highly inelastic event needed to produce an Ω^{-} in a $Y-N$ reaction. However, the high spark multiplicity of this event does not permit its unambiguous interpretation. Using a Monte Carlo calculation of our acceptance we find that one event would correspond to an Ω^{-} production cross section of $115 \mu\text{b}/\text{nucleon}$ if it were caused by an incident Ξ^{-} , and $1 \mu\text{b}/\text{nucleon}$ if caused by a Σ^{-} . The corresponding 90% confidence limits are $\sigma < 450 \mu\text{b}/\text{nucleon}$ and $\sigma < 5 \mu\text{b}/\text{nucleon}$, respectively.

We wish to thank our engineers, Satish Dhawan, Cordon Kerns, and Blaise Lombardi, and our technicians, Jon Blomquist, Ed Steigmeyer, Alan Wandersee, and Ralph Berner, for their help in the design and setup of the apparatus. We also thank the AGS staff, in particular David Berley, for providing the technical support needed for the success of this experiment.

*Present address: Dépt. de Physique Nucléaire et Corpusculaire, Université de Genève, Geneva, Switzerland.

†Present address: CERN, 1211 Geneva 23, Switzerland.

‡Research supported by the United States Atomic Energy Commission under Contract No. AT(11-1).

§Operated by Universities Research Association, Inc. under contract with the United States Atomic Energy Commission.

|| Work supported by the United States Atomic Energy Commission.

¶Present address: Brookhaven National Laboratory, Upton, New York 11973.

**Present address: Bell Laboratories, Holmdell, New Jersey 07733.

††Work supported in part by the National Science Found-

ation.

¹W. Hungerbühler *et al.*, Nucl. Instrum. Methods **115**, 221 (1974).

²W. J. Willis *et al.*, Nucl. Instrum. Methods **91**, 33 (1971).

³With an index of refraction of 1.000516.

⁴R. T. Deck, Phys. Rev. Lett. **13**, 169 (1964).

⁵V. Hungerbühler *et al.*, Phys. Rev. Lett. **24**, 1234 (1973).

⁶W. Tanenbaum *et al.*, Phys. Rev. Lett. **33**, 175 (1974).

⁷A. L. Kane, Acta Phys. Pol. **B3**, 845 (1972).

⁸H. J. Lipkin, Phys. Rev. D **7**, 846 (1973).

⁹Brandeis-Maryland-Syracuse-Tufts Collaboration, in *Hyperon Resonances 70: Proceedings of 1970 Duke Conference*, edited by E. C. Fowler (Moore, Durham, N. C., 1970), p. 317.

PHYSICAL REVIEW D

VOLUME 10, NUMBER 7

1 OCTOBER 1974

$\pi^+\pi^+ \rightarrow \pi^+\pi^+$ scattering below 0.7 GeV from $\pi^+p \rightarrow \pi^+\pi^+n$ at 5 GeV/c

J. P. Prukop, O. R. Sander, J. A. Poirier, C. A. Rey, A. J. Lennox, B. C.-j. Chen, N. N. Biswas,
N. M. Cason, V. P. Kenney, and W. D. Shephard
*Department of Physics, University of Notre Dame, Notre Dame, Indiana 46556**

R. D. Klem and I. Spirn
Argonne National Laboratory, Argonne, Illinois 60439†
(Received 22 April 1974)

Magnetostrictive spark chambers were used with a large magnet spectrometer to study the reaction $\pi^+p \rightarrow \pi^+\pi^+n$ at 5.0 GeV/c at Argonne National Laboratory. We measured differential cross sections for this reaction in the region of low nucleon momentum transfer and by extrapolation obtained cross sections and phase shifts for the reaction $\pi^+\pi^+ \rightarrow \pi^+\pi^+$ in the region of dipion mass less than 0.7 GeV. Effects of the interference between the strong $\pi^+\pi^+$ amplitude and the Coulomb amplitude off the mass shell were investigated and were found to be small. The S-wave phase shifts for $\pi^+\pi^+$ scattering near threshold were parameterized in terms of a scattering length, a_2 , and an effective range, r_2 ; the D wave by a scattering parameter, b_2 . The fits obtained by extrapolation techniques were insensitive to b_2 and gave $a_2 = -0.24 \pm 0.02$ F and $r_2 = -1.0 \pm 1.7$ F, where the error quoted is statistical. The fits obtained by off-shell fitting gave $a_2 = -0.22 \pm 0.04$ F, $r_2 = -0.34^{+0.9}_{-1.2}$ F, and $b_2 = -0.0041^{+0.0025}_{-0.0021}$ F⁵. These results for a_2 are inconsistent with a number of theoretical calculations.

I. INTRODUCTION

The scattering of pions from pions is the simplest example of a strong interaction amplitude and is, therefore, very fundamental. Its simplicity is due in part to the facts that the pion has no spin, obeys Bose-Einstein statistics, has a short-range force, and at low energy has but few partial waves. Because of the light mass of the pion it has the longest range of the hadrons and thus the one-pion-exchange mechanism dominates in many reactions. Thus an understanding of the $\pi\pi$ interaction is important not only in itself but for the understanding of many other reactions as well. The $\pi^+\pi^+$ interaction is particularly simple

because it is in the pure isotopic spin state $I=2$ and is not complicated by the presence of inelastic channels for energies less than four times the pion mass.

As there is at present no direct way to study the $\pi^+\pi^+$ interaction, we have chosen to explore the dipion system in the reaction $\pi^+p \rightarrow \pi^+\pi^+n$. By assuming the dominance of the one-pion-exchange mechanism (OPE) the $\pi^+p \rightarrow \pi^+\pi^+n$ cross section is related to the cross section for the scattering of a beam pion by the exchanged pion. The exchanged (virtual) pion is off the mass shell by an amount $\Delta^2 + \mu^2$, where μ is the pion rest mass and Δ^2 is the square of the momentum transfer between the incoming proton and outgoing neutron. The $\pi^+\pi^+$